Control of Emission by Intermolecular Fluorescence Resonance Energy Transfer and Intermolecular Charge Transfer

ARTICLE *in* THE JOURNAL OF PHYSICAL CHEMISTRY A · JUNE 2006

Impact Factor: 2.69 · DOI: 10.1021/jp060275m · Source: PubMed

Control of Emission by Intermolecular Fluorescence Resonance Energy Transfer and Intermolecular Charge Transfer

Mengtao Sun,*,† Tõnu Pullerits,† Pär Kjellberg,† Wichard J. D. Beenken,‡ and Keli Han§

Department of Chemical Physics, Lund University, Lund SE22100, Sweden, Department of Theoretical Physics I, Technische Universität Ilmenau, Postfach 100565, 98684 Ilmenau, Germany, and State Key Laboratory of Molecular Reaction Dynamics, Dalian Institute of Chemical Physics, Chinese Academy of Sciences, Dalian, 116023, P. R. China

Received: January 15, 2006; In Final Form: March 28, 2006

Control of emission by intermolecular fluorescence resonant energy transfer (IFRET) and intermolecular charge transfer (ICT) is investigated with the quantum-chemistry method using two-dimensional (2D) and three-dimensional (3D) real space analysis methods. The work is based on the experiment of tunable emission from doped 1,3,5-triphenyl-2-pyrazoline (TPP) organic nanoparticles (Peng, A. D.; et al. *Adv. Mater.* **2005**, *17*, 2070). First, the excited-state properties of the molecules, which are studied (TPP and DCM) in that experiment, are investigated theoretically. The results of the 2D site representation reveal the electron−hole coherence and delocalization size on the excitation. The results of 3D cube representation analysis reveal the orientation and strength of the transition dipole moments and intramolecular or intermolecular charge transfer. Second, the photochemical quenching mechanism via IFRET is studied (here "resonance" means that the absorption spectrum of TPP overlaps with the fluorescence emission spectrum of DCM in the doping system) by comparing the orbital energies of the HOMO (highest occupied molecular orbital) and the LUMO (lowest unoccupied molecular orbital) of DCM and TPP in absorption and fluorescence. Third, for the DCM−TPP complex, the nonphotochemical quenching mechanism via ICT is investigated. The theoretical results show that the energetically lowest ICT state corresponds to a pure HOMO−LUMO transition, where the densities of the HOMO and LUMO are strictly located on the DCM and TPP moieties, respectively. Thus, the lowest ICT state corresponds to an excitation of an electron from the HOMO of DCM to the LUMO of TPP.

I. Introduction

The resonance energy transfer between molecules, or between chromophores within a large molecule, plays a central role in many areas of modern chemistry and physics.[1] For example, doping techniques leading to intermolecular fluorescence resonance energy transfer (IFRET) have been proven to be an effective way to improve the luminescence efficiency and tune the emission color of electroluminescent material.[2,3] IFRET is a photophysical effect where energy that is absorbed by one fluorescent molecule (donor) is transferred nonradiatively to another fluorescent molecule (acceptor). The result is the decrease of lifetime and the quenching of fluorescence of donor species and the concomitant increase of fluorescence intensity of acceptor species. The efficiency of IFRET depends on the electronic coupling between the chromophores and the nuclear overlap integral (Franck−Condon factor). The latter together with the energy conservation principle leads to the overlap between the donor fluorescence spectrum and the acceptor absorption spectrum.[4] The energy-transfer rate can be expressed as [5]

$$k_{\mathrm{IFRET}} = \frac{K^2}{\tau_0}\left(\frac{R_0}{R}\right)^6 \tag{1}$$

where τ_0 is the radiative lifetime at the donor excited state, R is the distance between the fluorophores, and R_0 is the Förster radius. The orientation factor is defined as

$$K^2 = (\cos\theta_{\mathrm{T}} - 3\cos\theta_{\mathrm{D}}\cos\theta_{\mathrm{A}})^2 \tag{2}$$

where θ_{T} is the angle between the donor emission transition moment and the acceptor absorption transition moment and θ_{D} and θ_{A} are the angles between the donor−acceptor connection line and the donor emission and the acceptor absorption transition moments, respectively. The Förster radius is maximized when the host emission and the guest absorption exhibit good spectral overlap. The degree of overlap can be written as an integral

$$J = \int_0^\infty f_{\mathrm{D}}(\lambda)\epsilon_{\mathrm{A}}(\lambda)\lambda^4\,\mathrm{d}\lambda \tag{3}$$

where λ is the wavelength of the light, $\epsilon_{\mathrm{A}}(\lambda)$ is the molar extinction coefficient of the acceptor, and $f_{\mathrm{D}}(\lambda)$ is the normalized fluorescence spectrum of the donor.

The nonphotochemical quenching via intermolecular charge transfer (ICT) also plays an important role in many areas of chemistry and physics, such as in the fields of dye-sensitized solar cells (DSSCs) and photosynthetic reaction centers.[6−10] From the point of view of quantum chemistry, in an ICT state, an electron is transferred from one orbital i of a donor to an orbital j of an acceptor. As a result, a hole appears on the donor and an extra electron is localized on the acceptor.[6] The excitation

* To whom correspondence should be addressed. E-mail: Mengtao.Sun@chemphys.lu.se; mengtaosun@hotmail.com.
† Lund University.
‡ Technische Universität Ilmenau.
§ Dalian Institute of Chemical Physics.

10.1021/jp060275m CCC: $33.50
Published on Web 04/25/2006

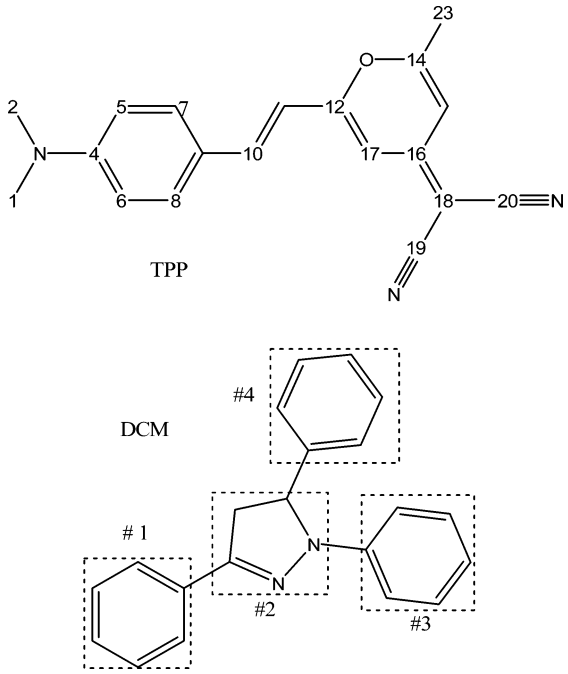

Figure 1. Chemical structure of TPP and DCM. The atoms in TPP and the molecular groups in DCM are labeled. The following figures use the same labeling.

energy of the ICT state can be expressed as[11]

$$E_{\mathrm{ICT}}(R) = E_{\mathrm{IP}} + E_{\mathrm{EA}} - \frac{e^2}{R} \tag{4}$$

where E_{IP} is the ionization potential of the donor, E_{EA} is the electron affinity of acceptor, and e^2/R is the electrostatic attraction between separated charges. The ground state and the excited ICT state wave functions can be written as[12]

$$\Psi_g = a\Psi_0(\mathrm{DA}) + b\Psi_1(\mathrm{D^+A^-}) \tag{5.a}$$

$$\Psi_e = a\Psi_1(\mathrm{D^+A^-}) - b\Psi_0(\mathrm{DA}) \tag{5.b}$$

where $\Psi_0(\mathrm{DA})$ is the configuration for the normal, weakly bound complex and $\Psi_1(\mathrm{D^+A^-})$ is the CT configuration. For weakly bound complexes, $b \ll a$ and little charge is transferred from the donor to the acceptor in the ground state. The transition dipole moment for the ICT transition in a weak complex can be approximated as $V_{\mathrm{eg}} \approx a^*b\mu_{11} + aa^*\mu_{01}$,[13] where μ_{11} is the static dipole moment of the ion pairs in the ICT configuration and μ_{01} is the transition dipole $\langle\Psi_1|\mu|\Psi_0\rangle$.

To visually inspect the spatial distribution of the excitation for large conjugated polymers, several elaborate theoretical methods have been developed. One is the two-dimensional (2D) site representation of the transition density matrix,[14−18] which is employed to analyze the electron−hole coherence and the excitation delocalization in conjugated molecules. In addition, the three-dimensional (3D) cube representation of the transition density (TD)[18−27] and the charge difference density (CDD)[18,20−27] have been used to analyze the charge and energy transfer in several conjugated polymers.[18−27]

To interpret theoretically the experiment of tunable emission from doped 1,3,5-triphenyl-2-pyrazoline (TPP) organic nanoparticles,[2] the theoretical model of controlling the emission by intermolecular charge and energy transfer in the DCM−TPP complexes (see Figure 1) is presented in this paper. The article is organized as follows. In section II, the theoretical approaches

TABLE 1: Calculated Absorption and Fluorescence Wavelengths (nanometers) and Their Corresponding Oscillator Strengths (in the parentheses) for DCM, TPP, and the DCM−TPP Complex

	DCM			TPP	TPP−DCM
	absorption		fluorescence	absorption	absorption
S_1	361 (0.56)[a]	***361* (*0.57*)**	424 (0.57)	**437 (1.13)**	509 (0.00)
S_2					**448 (1.60)**
S_3					385 (0.03)
S_4					376 (0.05)
S_5					***367* (*0.42*)**

[a] Calculated with Turbomole 5.71 and other theoretical results were calculated with Gaussian 03.

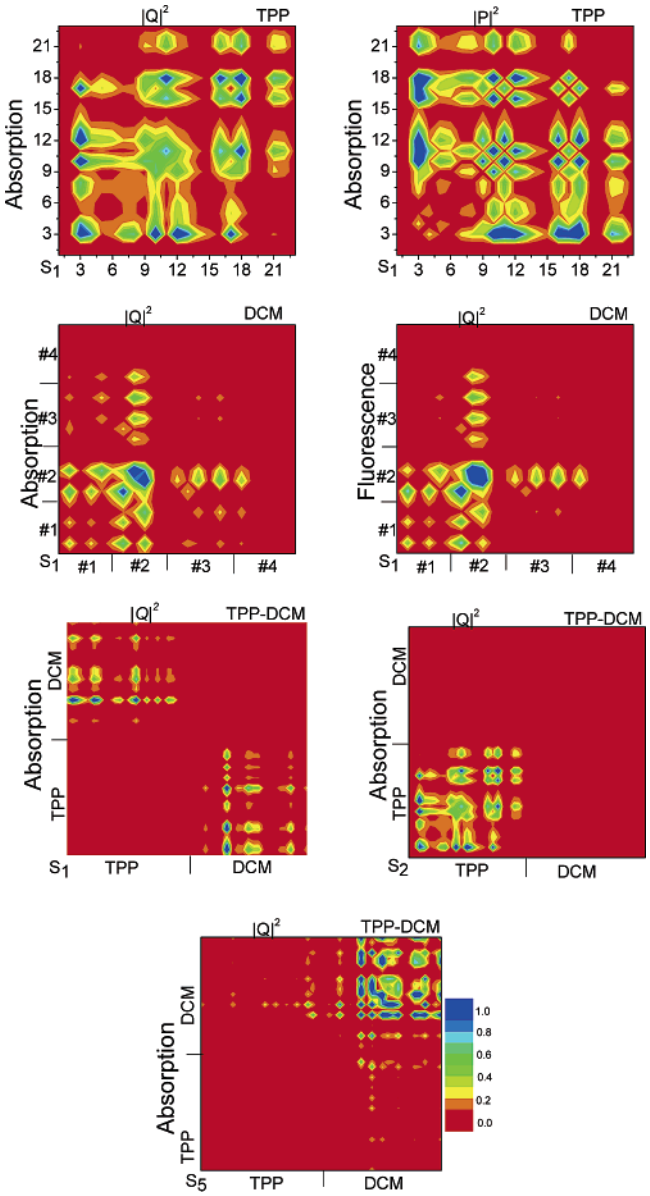

Figure 2. Contour plots of transition density matrixes corresponding to the $|Q|^2$ and $|P|^2$ operators of DCM, TPP, and the DCM−TPP complex in absorption and fluorescence. Transitions correspond to the states indicated in the lower left corners of the plots.

are described. In section III, the excited-state properties of DCM and TPP are studied with quantum-chemistry methods as well as 2D and 3D real space analyses. In section IV, the quenching mechanisms of the DCM fluorescence are analyzed. We point out a possibility of quenching via ICT by studying the excited-state properties of the DCM−TPP complex, where the first

excited state is the ICT state. In section V, a short conclusion closes the presentation.

II. Method

The ground-state geometry optimizations of DCM, TPP, and the DCM−TPP complex were performed, using density functional theory (DFT)[28] with Becke's three-parameter hybrid exchange functional with Lee−Yang−Parr gradient-corrected correlation functional (B3LYP functional)[29] at the 6-31G basis level. The molecular geometry of the lowest excited state was optimized at the configuration interaction singles (CIS)/STO-3G level.[30] No constraints to bonds/angles/dihedral angles were applied in the calculations, and all atoms were free to be optimized. The excited-state electronic structures were calculated using time-dependent density functional theory (TD-DFT)[31] with the B3LYP/6-31G method. All of the above quantum-chemical calculations were performed with the Gaussian 03 suite of programs.[32] At the excited-state optimal geometry, the transition frequency and oscillator strength correspond to the vertical fluorescence.[33−35] Absorption and fluorescence points were treated at the TD-B3LYP/6-31G//B3LYP/6-31G and TD-B3LYP/6-31G//CIS/STO-3G levels, respectively, in conventional quantum-chemical notation "single point//optimization level".[33−35]

The geometry optimizations of DCM for the ground state were also performed with the DFT method using the B3LYP_Gaussian functional and SV(P) basis set. The excited-state electronic structures were also calculated by the TD-DFT method B3LYP functional, and SV(P) basis set, using Turbomole Suite.[36]

2D Site Representations. The exciton coordinate and momentum operators can be defined as[14,18,26]

$$Q_\lambda = \sum_{u,o} \alpha_{u,o}^{\lambda} \sum_{m,n} (a_{n,u}^{+} a_{m,o} + a_{m,u}^{+} a_{n,o}) \tag{6}$$

and

$$P_\lambda = \sum_{u,o} \alpha_{u,o}^{\lambda} \sum_{m,n} (a_{n,u}^{+} a_{m,o} - a_{m,u}^{+} a_{n,o}) \tag{7}$$

where $a_{n,u}^{+}$ ($a_{n,o}$) are the creation and annihilation operators for the unoccupied (u) and occupied (o) molecular orbitals for the exciton at site (atom) n. The coefficient $\alpha_{u,o}^{\lambda}$ is the configuration interaction (CI) coefficient of the $o \rightarrow u$ transition to the λth excited state. When $n \neq m$, eq 6 represents the exciton coherence and eq 7 represents the oscillation of the electron−hole pair between orbitals n and m.[18,26] When $n = m$, $Q_\lambda = 2 \sum_{u,o} \alpha_{u,o}^{\lambda} \sum_n a_{n,u}^{+} a_{n,o}$ determines the corresponding transition density and $P_\lambda = 0$. For 2D site representation of the exciton coordinate and momentum, we use the reduced matrices

$$|Q_\lambda|^2$$

and

$$|P_\lambda|^2 \tag{8}$$

respectively.[14] Thus, $|P_\lambda|^2$ describes the oscillation of the electron and hole from the atomic sites n to m and vice versa, while $|Q_\lambda|^2$ is a measure of the delocalization of the exciton as a whole for the transition from the ground state to the λth excited state.[26]

3D Cube Representation. When $n = m$ in eq 6, the coordinate operator leads to the transition density in 3D cube representation.[20] The transition density $\rho_{\lambda 0}$ contains information about the spatial location of the excitation[22] and is directly related to the transition dipole

$$\mu_{\lambda,0} = e \int r \rho_{\lambda 0}(r)\, \mathrm{d}^3 r \tag{9}$$

Furthermore, it is of particular relevance for excitonic interaction at shorter distances.[20] Besides the transition density, the charge difference density (CDD) between the ground and the excited states can also be calculated.[21]

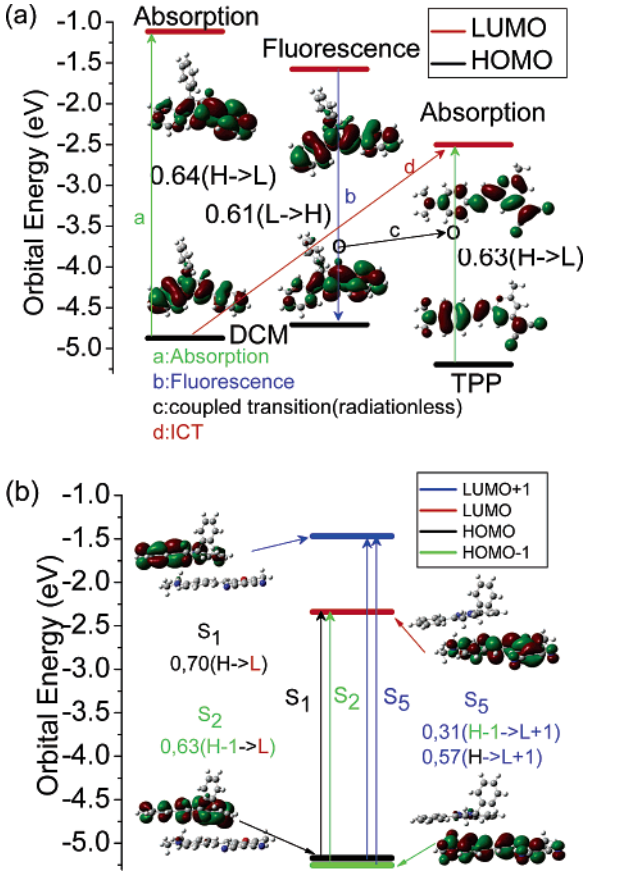

Figure 3. Molecular orbital energies and densities of the HOMOs and LUMOs of DCM, TPP, and the DCM−TPP complex, where the CI main coefficients of orbital transitions are shown. We point out that the squares of all CI coefficients of a transition add up to 0.5.

III. Excited-state Properties of DCM and TPP

The calculated absorption and fluorescence frequencies and oscillator strengths of DCM and TPP are listed in Table 1. The results are in good agreement with the experimental data.[2] Figure 2. shows the contour plots representing the $|Q_1|^2$ and $|P_1|^2$ for DCM and TPP in absorption and fluorescence. The contour plots of TPP show that excitation is delocalized over the whole molecule. The $|Q_1|^2$ and $|P_1|^2$ plots are not significantly different. The physical meaning of the differences between $|Q_1|^2$ and $|P_1|^2$ has been discussed in another study of excited-state properties of neutral and charged conjugated polymers and oligomers.[26] For example, the electron−hole coherence of a nitrogen atom #3 is rather high for atoms #4, #10, #12, #13, and #17 seen in the $|Q_1|^2$ plot, while electron−hole oscillations occur between #3 N and atoms #10−#12, #16−#18, #21, and #22 according to the $|P_1|^2$ plot. For DCM and the TTP−DCM complex, only $|Q_1|^2$ plots are presented. In DCM, one can clearly see that unit #4 is not involved in the excited state. The plots of absorption and fluorescence for DCM are very similar indicating that the excitation does not localize significantly. In conjugated polymers

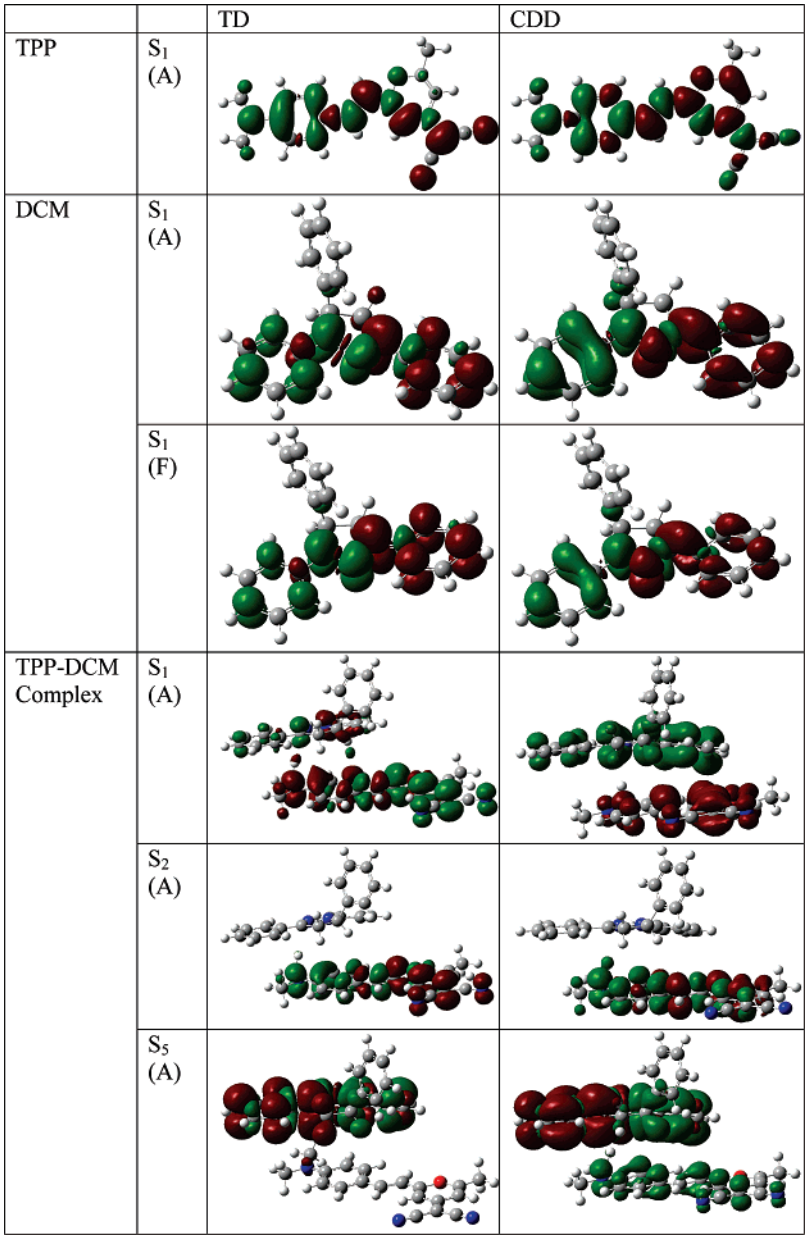

Figure 4. Transition densities (TDs) and charge difference densities (CDDs) of TPP, DCM, and the DCM−TPP complex in absorption (A) and fluorescence (F), where the green and the red stand for the hole and electron, respectively.

such as PPV, the electron−hole coherence in fluorescence is substantially localized compared with the absorption.[16]

For DCM and TPP, the S_1 state is almost a purely HOMO to LUMO transition in both absorption and fluorescence. The energies and the corresponding orbital distributions for the HOMO and LUMO together with the CI coefficients can be seen in Figure 3a. As expected, the HOMO−LUMO energy gap is higher in absorption than in fluorescence, so the absorption frequency is larger than the fluorescence frequency.[35] From Figure 3a, for DCM, the HOMO is mainly distributed over #1 and #2, while the LUMO is mainly on #2 and #3. Consequently, we expect that the HOMO to LUMO transition would lead to a charge transfer from #1 to #3, while #2 acts as a bridge. The CDDs and TDs of the molecules are shown in the Figure 4. Indeed, the CDD of DCM confirms the above-expected trend. From the TDs, one can get a good idea about the orientation of the transition dipole moments. For TPP, it is oriented along the π-conjugation of the molecule, and for DCM, it is oriented from group #1 to group #3. There is no significant difference between the absorption and fluorescence TDs and CDDs for DCM.

IV. DCM Fluorescence Quenching Mechanisms

The general condition of the energy transfer is that the transition energy of the donor fluorescence has to mach the energy of the acceptor absorption reasonably well. From Figure 3a, one can see that this is indeed the case, and from Figure 3b, we expect an efficient donor fluorescence quenching via IFRET provided that the mutual orientation of the molecules leads to a sufficiently high orientation factor K.

The calculated absorption frequencies and the oscillator strengths of the DCM−TPP complex are listed in Table 1. The second and the fifth excited states have strong oscillator strengths. Inspection of the electron−hole correlation maps (Figure 2), the molecular orbitals which correspond to the transitions (Figure 3b), and the TDs (Figure 4) show that these states are almost purely TPP and DCM molecular transitions. The first singlet excited state has zero transition strength. The

molecular orbitals, electron−hole correlation maps, and CDD clearly show that this state is an ICT state.

From the above results, we conclude that the emission of DCM is controlled not only by IFRET but also by ICT. This ICT excited state can also be considered as a dissociated exciton state, where the electron promoted in the LUMO level of the excited donor (L_D) can be transferred to the lower-lying LUMO level of the acceptor (L_A), with the hole remaining on the HOMO level of the donor, thereby forming a polaron pair. Thus, this photoinduced *electron-transfer* process has converted light into charges. Note that the same final charge-separated state can be reached when the acceptor is initially photoexcited, following a photoinduced *hole-transfer* process from the HOMO level of the acceptor (H_A) to the HOMO level of the donor (H_D). Our theoretical findings indicate that the studied materials may be interesting from the point of view of optoelectronic devices such as solar cells and photodiodes.

V. Conclusion

The theoretical model of controlling the emission by intermolecular charge and energy transfer has been presented. The study is based on the experiment of tunable emission from doped 1,3,5-triphenyl-2-pyrazoline organic nanoparticles. We show that the IFRET is not the only quenching channel and propose that a significant part of the DCM fluorescence can be quenched by ICT.

Acknowledgment. This work was supported by the National Natural Science Foundation of China (Grant Nos. 10374040 and 20573110), the Swedish Research Council, and the Wenner-Gren Foundation of Sweden.

References and Notes

(1) Andrews, D. L.; Demidov, A. A. *Resonance Energy Transfer*; Wiley: New York, 1999.

(2) Peng, A. D.; Xiao, D. B.; Ma, Y.; Yang, W. S.; Yao, J. N. *Adv. Mater.* **2005**, *17*, 2070.

(3) Pompa, P. P.; Chiuri, R.; Manna, L.; Pellegrino, T.; del Mercato, L. L.; Parak, W. J.; Calabi, F.; Cingolani, R.; Rinaldi, R. *Chem. Phys. Lett.* **2006**, *417*, 351.

(4) Van Der Meer, B. W.; Coker, G., III; Chen, S. Y. *Resonance Energy Transfer Theory and Data*; VCH: New York, 1994.

(5) Scholes, G. D. *Annu. Rev. Phys. Chem.* **2003**, *54*, 57.

(6) Sun, M. T.; Li, Y. Z.; Ma, F. C. *Chem. Phys. Lett.* **2005**, *412*, 425.

(7) Wang, X. F.; Xiang, J. F.; Wang, P.; Koyama, Y.; Yanagida, S.; Wada, Y.; Hamada, K.; Sasaki, S.; Tamiaki, H. *Chem. Phys. Lett.* **2005**, *408*, 409.

(8) Xiang, J. F.; Rondonuwu, F. S.; Kakitani, Y.; Fujii, R.; Watanabe, Y.; Koyama, Y. *J. Phys. Chem. B* **2005**, *109*, 17066.

(9) Dreuw, A.; Fleming, G. R.; Head-Gordon, M. *J. Phys. Chem. B* **2003**, *107*, 6500.

(10) Vaswani, H. M.; Hsu, C. P.; Head-Gordon, M.; Fleming, G. R. *J. Phys. Chem. B* **2003**, *107*, 7940.

(11) Dreuw, A.; Weisman, J. L.; Head-Gordon, M. *J. Chem. Phys.* **2003**, *119*, 2943.

(12) Mulliken, R. S.; Person, W. B. *Molecular Complexes*, 1st ed.; Wiley-Interscience: NewYork, 1969.

(13) DeBoer, G.; Preszler Prince, A.; Young, M. A. *J. Chem. Phys.* **2001**, *115*, 3112.

(14) Mukamel, S.; Tretiak, S.; Wagersreiter, T.; Chernyak, V. *Science* **1997**, *277*, 781.

(15) Zojer, E.; Buchacher, P.; Wudl, F.; Cornil, J.; Calbert, J. Ph.; Bredas, J. L. Leising, G. *J. Chem. Phys.* **2000**, *113*, 10002.

(16) Tretiak, S.; Saxena, A.; Martin, R. L.; Bishop, A. R. *Phys. Rev. Lett.* **2002**, *89*, 097402.

(17) Tretiak, S.; Mukamel, S. *Chem. Rev.* **2002**, *102*, 3171.

(18) Sun, M. T. *J. Chem. Phys.* **2006**, *124*, 054903.

(19) Krueger, B. P.; Scholes, G. D.; Fleming, G. R. *J. Phys. Chem. B* **1998**, 102, 5378.

(20) Beenken, W. J. D.; Pullerits, T. *J. Chem. Phys.* **2004**, *120*, 2490.

(21) Beenken, W. J. D.; Pullerits, T. *J. Phys. Chem. B.* **2004**, *108*, 6164.

(22) Jespersen, K. G.; Beenken, W. J. D.; Zaushitsyn, Y.; Yartsev, A.; Andersson, M.; Pullerits, T.; Sundström, V. *J. Chem. Phys.* **2004**, *121*, 12613.

(23) Sun, M. T.; Kjellberg, P.; Ma, F. C.; Pullerits, T. *Chem. Phys. Lett.* **2005**, *401*, 558.

(24) Persson, N. K.; Sun, M. T.; Kellberg, P.; Pullerits, T.; Inganäs, O. *J. Chem. Phys.* **2005**, *123*, 204718.

(25) Sun, M. T.; Chen, Y. H.; Song, P.; Ma, F. C. *Chem. Phys. Lett.* **2005**, *413*, 110.

(26) Sun, M. T.; Kjellberg, P.; Beenken, W. J. D.; Pullerits, T. *Chem. Phys.* Submitted for publication.

(27) Sun, M. T.; Song, P.; Chen, Y. H.; Ma, F. C. *Chem. Phys. Lett.* **2005**, *416*, 94.

(28) Dreizler, M. R.; Gross, E. K. U. *Density Functional Theory*; Springer Verlag: Heidelberg, Germany, 1990.

(29) Lee, C.; Yang, W.; Parr, R. G. *Phys. Rev. B* **1988**, *37*, 785.

(30) Foresman, J. B.; Head-Gordon, M.; Pople, J. A.; Frisch, M. J. *J. Phys. Chem.* **1992**, *96*, 135.

(31) Gross, E. K. U.; Kohn, W. *Phys. Rev. Lett.* **1985**, *55*, 2850.

(32) Frisch, M. J.; Trucks, G. W.; Schlegel, H. B.; Scuseria, G. E.; Robb, M. A.; Cheeseman, J. R.; Montgomery, J. A., Jr.; Vreven, T.; Kudin, K. N.; Burant, J. C.; Millam, J. M.; Iyengar, S. S.; Tomasi, J.; Barone, V.; Mennucci, B.; Cossi, M.; Scalmani, G.; Rega, N.; Petersson, G. A.; Nakatsuji, H.; Hada, M.; Ehara, M.; Toyota, K.; Fukuda, R.; Hasegawa, J.; Ishida, M.; Nakajima, T.; Honda, Y.; Kitao, O.; Nakai, H.; Klene, M.; Li, X.; Knox, J. E.; Hratchian, H. P.; Cross, J. B.; Bakken, V.; Adamo, C.; Jaramillo, J.; Gomperts, R.; Stratmann, R. E.; Yazyev, O.; Austin, A. J.; Cammi, R.; Pomelli, C.; Ochterski, J. W.; Ayala, P. Y.; Morokuma, K.; Voth, G. A.; Salvador, P.; Dannenberg, J. J.; Zakrzewski, V. G.; Dapprich, S.; Daniels, A. D.; Strain, M. C.; Farkas, O.; Malick, D. K.; Rabuck, A. D.; Raghavachari, K.; Foresman, J. B.; Ortiz, J. V.; Cui, Q.; Baboul, A. G.; Clifford, S.; Cioslowski, J.; Stefanov, B. B.; Liu, G.; Liashenko, A.; Piskorz, P.; Komaromi, I.; Martin, R. L.; Fox, D. J.; Keith, T.; Al-Laham, M. A.; Peng, C. Y.; Nanayakkara, A.; Challacombe, M.; Gill, P. M. W.; Johnson, B.; Chen, W.; Wong, M. W.; Gonzalez, C.; Pople, J. A. *Gaussian 03*, revision B.05; Gaussian, Inc.: Pittsburgh, PA, 2003.

(33) Katan, C.; Terenziani, F.; Mongin, O.; Werts, M. H. V.; Porrès, L.; Pons, T.; Mertz, J.; Tretiak, S.; Blanchard-Desce, M. *J. Phys. Chem. A* **2005**, *109*, 3024.

(34) Masunov, A.; Tretiak, S.; Hong, J. W.; Liu, B.; Bazan, G. C. *J. Chem. Phys.* **2005**, *122*, 224505.

(35) Sun, M. T. *Chem. Phys.* **2006**, *320*, 155.

(36) Ahlrichs, R.; et al. *Turbomole 5.71*; The Quantum Chemistry Group, University of Karlsruhe: Karlsruhe, Germany, 2005.